frontiers | Frontiers in Nutrition

ORIGINAL RESEARCH
published: 30 June 2022
doi: 10.3389/fnut.2022.921758

Liver Transcriptome and Gut Microbiome Analysis Reveals the Effects of High Fructose Corn Syrup in Mice

Yu Shen[1,2†], *Yangying Sun*[1†], *Xiaoli Wang*[2], *Yingping Xiao*[2], *Lingyan Ma*[2], *Wentao Lyu*[2], *Zibin Zheng*[2], *Wen Wang*[2*] and *Jinjun Li*[3*]

[1] State Key Laboratory for Managing Biotic and Chemical Threats to the Quality and Safety of Agro-products, College of Food and Pharmaceutical Sciences, Ningbo University, Ningbo, China, [2] Institute of Agro-product Safety and Nutrition, Zhejiang Academy of Agricultural Sciences, Hangzhou, China, [3] Institute of Food Sciences, Zhejiang Academy of Agricultural Sciences, Hangzhou, China

OPEN ACCESS

Edited by:
Jie Yin,
Hunan Agricultural University, China

Reviewed by:
Shimeng Huang,
China Agricultural University, China
Daxi Ren,
Zhejiang University, China

***Correspondence:**
Wen Wang
ww_hi1018@163.com
Jinjun Li
lijinjun@zaas.ac.cn

[†] *These authors have contributed equally to this work*

Specialty section:
This article was submitted to Nutrition and Microbes, a section of the journal Frontiers in Nutrition

Received: *16 April 2022*
Accepted: *01 June 2022*
Published: *30 June 2022*

Citation:
Shen Y, Sun Y, Wang X, Xiao Y, Ma L, Lyu W, Zheng Z, Wang W and Li J (2022) Liver Transcriptome and Gut Microbiome Analysis Reveals the Effects of High Fructose Corn Syrup in Mice. Front. Nutr. 9:921758. doi: 10.3389/fnut.2022.921758

High fructose corn syrup (HFCS) is a viscous mixture of glucose and fructose that is used primarily as a food additive. This article explored the effect of HFCS on lipid metabolism-expressed genes and the mouse gut microbiome. In total, ten 3-week-old male C57BL/6J mice were randomly divided into two groups, including the control group, given purified water (Group C) and 30% HFCS in water (Group H) for 16 weeks. Liver and colonic content were collected for transcriptome sequencing and 16S rRNA gene sequencing, respectively. HFCS significantly increased body weight, epididymal, perirenal fat weight in mice ($p < 0.05$), and the proportion of lipid droplets in liver tissue. The expression of the ELOVL fatty acid elongase 3 (Elovl3) gene *was* reduced, while Stearoyl-Coenzyme A desaturase 1 (*Scd1*), peroxisome proliferator activated receptor gamma (*Pparg)*, fatty acid desaturase 2 (*Fads2*), acyl-CoA thioesterase 2 (*Acot2*), acyl-CoA thioesterase 2 (*Acot3*), acyl-CoA thioesterase 4 (*Acot4*), and fatty acid binding protein 2 (*Fabp2*) was increased in Group H. Compared with Group C, the abundance of Firmicutes was decreased in Group H, while the abundance of Bacteroidetes was increased, and the ratio of Firmicutes/Bacteroidetes was obviously decreased. At the genus level, the relative abundance of *Bifidobacterium*, *Lactobacillus*, *Faecalibaculum*, *Erysipelatoclostridium,* and *Parasutterella* was increased in Group H, whereas that of *Staphylococcus*, *Peptococcus*, *Parabacteroides*, *Donghicola,* and *Turicibacter was* reduced in Group H. *Pparg*, *Acot2*, *Acot3,* and *Scd1* were positively correlated with *Erysipelatoclostridium* and negatively correlated with *Parabacteroides*, *Staphylococcus,* and *Turicibacter*. *Bifidobacterium* was negatively correlated with *Elovl3*. Overall, HFCS affects body lipid metabolism by affecting the expression of lipid metabolism genes in the liver through the gut microbiome.

Keywords: gut microbiota, hepatic lipid metabolism, high fructose corn syrup, transcriptome analysis, mouse

INTRODUCTION

High fructose corn syrup (HFCS) is a viscous mixture of glucose and fructose. In recent years, due to the rising price of sugar, the low price and better taste of HFCS have been favored by the food industry, especially in beverage production, and it is also a key ingredient in baked goods, desserts, and juices (1). Fructose in the diet may contribute to increased energy intake and weight gain, which can lead to problems, such as obesity (2). Furthermore, an HFCS diet significantly alters the community structure of the gut microbiome and lipid metabolism (3, 4).

The liver is primarily the site of fructose metabolism, which is an essential organ in the body related to lipid metabolism (5, 6) and plays an important role in regulating appetite and body weight (7). Li et al. found that most of the changes in the liver transcriptome level of laying hens are closely related to fat metabolism by performing transcriptome analysis on the liver of young and laying hens (8). It was shown that peroxisome proliferator activated receptor gamma (*Pparg*) is a key factor in lipid formation and can be combined with specific substances to reduce lipid formation (9). Studies on broilers of the same breed and different body weights showed that the expression of *LIPG* and *CPT1A* genes is related to lipid metabolism (10, 11). Emmanuelle (12) adipose regulation in animals of different body sizes is related to the regulation of genes involved in adipogenesis. Furthermore, the expression of different genes in the organism may lead to differences in fat deposition (13).

The gut microbiome affects host lipid metabolism and plays an important role in the development of metabolic diseases through interaction with the diet (14, 15). The human gut contains a diverse and complex microbial community that plays an important role in energy and lipid metabolism (16). The gut microbiome is colonized by 10^{14} macroorganisms of numerous species, which are important components of the human gut microbiome ecosystem (17). The microbiome in the gastrointestinal tract of mice consists mainly of Firmicutes (74%) and Bacteroidetes (23%) at the phylum level (18). A high-fructose diet altered the Firmicutes/Bacteroidetes ratio and the abundance of *Parasutterella*, *Lactobacillus*, *Bifidobacteriaceae,* and *Alistipes* (19, 20). Crescenzo et al. (21) indicated that a fructose diet alters the mouse gut microbiome, which contributes to the dysregulation of liver metabolism.

Thus, to better understand the effects of HFCS intake on mouse metabolism, this study is aimed to determine the effects of HFCS intake on the gene expression of liver lipid metabolism and the community structure and function of the gut microbiome in mice and the association between the gene expression and the gut microbiome.

MATERIALS AND METHODS

Ethics Statement

The study was conducted at the Laboratory Animal Center of Zhejiang Academy of Agricultural Sciences (Animal Experimentation License No. 286868667) and was approved by the Zhejiang Provincial Ethics Committee for Laboratory Animals (Ethical Approval No. 78865576). All methods were conducted following the relevant guidelines and regulations.

Preparation of Animal and Liver Tissue Samples

Male C57BL/6J mice of 3-week-old were purchased from Shanghai Slack Company. After all mice were adaptively fed for 1 week, they were randomly divided into two groups, the control group (Group C) and the HFCS group (Group H), which were fed drinking water containing 30% HFCS. All mice were fed at room temperature and relative humidity of 50–70%. Each group was exposed to light for 12 h a day, and the mice were free to eat and drink. After 16 weeks of intervention, water was removed without fasting for 12 h. The mice were weighed, and the liver, epididymal fat, and perirenal fat were quickly weighed. To analyze the liver, the left leaf was placed in 4% paraformaldehyde, and the right leaf was stored at −80°C. Data were recorded in time for all operations. The liver samples for examination were fixed with 4% paraformaldehyde. After the fixed state was achieved, the samples were pruned, dehydrated, embedded, sectioned, stained, and sealed in strict accordance with the standard operating procedure (SOP) of the unit for pathological experiment detection and finally qualified for microscopic examination. The whole intestine was separated from the abdominal cavity of the mice, and the content of the colon was removed and stored on dry ice.

RNA Extraction

Total RNA was isolated from the liver tissues of 10 mice. TRIzol (Invitrogen, USA) was used to purify the extract, and the purity of RNA (ratio of OD260/280 and OD260/230) was detected by a Nano Spectrophotometer (Implen, Maryland, CA, USA). An Agilent 2100 Bioanalyzer (Agilent Technologies, Santa Clara, CA, USA) was used to accurately detect the integrity and total amount of RNA.

Library Construction and Sequencing

According to the manufacturer's suggestion, the kit used to build the library was the NEBNext® Ultra™ RNA Library Prep Kit for illumination. After the library was built, Qubit 2.0 Fluorometer was used for preliminary quantification, and the library was diluted to 1.5 ng/μl. Then, an Agilent 2100 Bioanalyzer was used to detect the insert size of the library. After the insert size met the expectation, quantitative real-time PCR (qRT-PCR) accurately quantified the effective concentration of the library (the effective concentration of the library was higher than 2 nM) to ensure the quality of the library. After library inspection was qualified, different libraries were pooled according to the requirements of effective concentration and target off-board data volume. Then, Illumina sequencing was performed, and a 150 bp paired-end reading was generated.

Differential Gene Expression Analysis

DESeq2 software (1.20.0) was used to analyze the differential expression between the two comparison combinations. DESeq2 provides statistical procedures for determining differential expression in digital gene expression data using a model based

TABLE 1 | Primers for RT-qPCR.

Gene	Size (bp)	Annealing (°C)	Forward (5′ to 3′)	Reword (5'to3')
GAPDH	127	60	GAAGGTCGGTGTGAACGGATTTG	CATGTAGACCATGTAGTTGAGGTCA
Scd1	110	60	GCAAGCTCTACACCTGCCTCTTC	CAGCCGTGCCTTGTAAGTTCTG
Pparg	133	60	CCAAGAATACCAAAGTGCGATCA	CCCACAGACTCGGCACTCAAT
Elovl3	91	60	GTAAGCGTCCACTCATCTTTGTC	CCCGAAGGCACTTTGTTCTTGTAT
Fads2	86	60	CGACATTTCCAACACCATGCCAA	CACTCGCCAAGGACAAACAC
Acot2	97	60	GACAGGGTTTCTCTGTGTACC	GTGGCTTTACTCCCAGCACTT
Acot3	121	60	CTGCTACATCCCTGGAGTTC	CCCTTAACTGCTGAGCCATCTTT
Acot4	178	60	GCCTGTAACAGACATGGTAGATTC	CTGTAACAAGCACAGGCTGGTA
Fabp2	73	60	CTGATTGCTGTCCGAGAGGTT	GCTTGGCCTCAACTCCTTCATAT

on a negative binomial distribution. Benjamini and Hochberg's method was used to adjust the p-value to control the error detection rate. Genes with an adjusted $p < 0.05$ found by DESeq2 were called differentially expressed genes (DEGs).

DEGs of Gene Oncology (GO) and Kyoto Encyclopedia Gene and Genome (KEGG) Enrichment Analyses

Gene Oncology enrichment analysis of DEGs was realized by Cluster Profiler (3.4.4) software, in which the gene length bias was corrected, and GO terms with corrected p-values <0.05 were significantly enriched by DEGs. We used Cluster Profiler (3.4.4) software analysis of DEGs in KEGG pathway enrichment after using a local version of the GSEA tool http://www.broadinstitute.org/gsea/index. jsp, GO to the species, KEGG GSEA datasets. The KEGG (http://www.genome.jp/KEGG/) (22) information from the molecular level, especially the genome sequencing high flux experimental technology of large-scale molecular datasets, understands cells, biological, ecological system, the advanced features of biological systems, and the utility of the database resources. In this study, KOBAS (23) software was used to test the statistical enrichment of DEGs in the KEGG pathway.

RT-QPCR Analysis

To confirm the reproducibility and accuracy of the RNA sequencing (RNA-Seq) gene expression data obtained from mouse liver libraries, RT-qPCR analysis was performed. The RT-qPCR system (20 μl) was as follows: Power SYBR® Green Master Mix, 10 μl; gene-specific upstream and downstream primers (10 μmol/L), 0.5 μl; sterile water, 8 μl; and cDNA template, 1 μl. The reaction conditions were as follows: 95°C for 1 min, followed by 40 cycles of 95°C for 15 s and 63°C for 25 s (for collecting fluorescence data). The relative expression level of each gene was determined by the 2^{-Ct} method using GAPDH as the internal reference gene, and the reaction was repeated three times for each sample. The primers used for quantification in the study were designed using the Primer-Basic Local Alignment Search Tool (BLAST) on the NCBI website (https://www.ncbi.nlm.nih.gov/tools/primer-blast/). Gene information for RT-PCR is shown in **Table 1**.

Histological Staining

The histological morphology of the liver was observed using hematoxylin-eosin staining. After fixation with 4% paraformaldehyde and in good condition, the samples were pruned, dehydrated, embedded, sectioned, stained, and sealed in strict accordance with the procedures of the unit's pathological experiment detection SOP and finally qualified for microscopic examination. Steatosis of liver tissue in mice treated with 30% HFCS was observed.

DNA Extraction and Sequencing

According to the instructions of the manufacturer, microbial genomic DNA was obtained from each intestinal content (QIAamp DNA Stool Mini Kit QIAGEN, CA, USA). The barcode-specific primers 515 F 5′-barcode-GTGCCAGCMGCCGCGG-3′ and 907 R 5′-CCGTCAATTCMTTTRAGTTT-3′ were synthesized to amplify the V4+V5 region of 16S rRNA gene sequencing (24). The PCRs were performed in triplicate using a 20 μl mixture that contained 4 μl of 5 × FastPfu Buffer, 2 μl of 2.5 mM deoxynucleotide triphosphates (dNTPs), 0.8 μl of forward primer (5 μM), 0.8 μl of reverse primer (5 μM), 0.4 μl of FastPfu Polymerase, 0.2 μl of bovine serum albumin (BSA), 10 ng of template DNA, and ddH_2O was added to 20 μl. Amplicons were extracted from 2% agarose gels and purified using the AxyPrep DNA Gel Extraction Kit (Axygen Biosciences, Union City, CA, USA) according to the manufacturer's instructions and quantified using a QuantiFluorTM-ST (Promega, USA) Bioinformatics Analysis Illumina paired reads that were multiplexed, and clean reads were screened in the Quantitative Analysis of Microbial Ecology (QIIME) quality filter (25), combined into labels using FLASH (26), and then allocated a unique barcode to each sample. After removing redundancy, the labels of each sample were analyzed, and UPARSE and UCHIME were used to assign unique labels with sequence similarity ≥97% to the same operational taxonomic unit (OTU). Selected OTUs were annotated with taxonomic information using the Ribosomal Database Project (RDP) classifier (27). Alpha diversity and beta diversity were calculated and visualized in GraphPad Prism 8.0.2 (San Diego, CA, USA).

Statistical Analysis

All the data were statistically analyzed by SPSS version 23 software using one-way ANOVA. The mean ± standard deviation (SD; $x \pm s$) is indicated, and $p < 0.05$ was considered statistically significant.

RESULTS

Body Weight and Fat Deposition in Mice

The average body weight of mice in Group C was 29.060 ± 0.446 g and that in Group H was 38.220 ± 1.515 g, and the difference between the two groups was extremely significant ($p < 0.001$; **Figure 1A**). The average weight of epididymal fat showed a significant increase in the H group, which was 1.886 ± 0.216 g, while the weight of epididymal fat in Group C was 0.762 ± 0.098 g ($p < 0.001$; **Figure 1B**). By comparing the perirenal fat of mice in the two groups, we found that the difference between the two groups was extremely significant, 0.284 ± 0.020 g in Group C and 0.732 ± 0.123 g in Group H ($p < 0.001$; **Figure 1C**). The results showed that the liver weight of mice in Group H was increased but not significantly different as compared to Group C, while the average liver weight of Group C was 1.152 ± 0.031 g and that of Group H was 1.364 ± 0.100 g ($p = 0.0778$; **Figure 1D**). Round vacuoles of varying sizes were observed in the cytoplasm, and larger areas of lipid droplets were observed in Group H than in Group C. As shown in **Figures 1E–H**, it

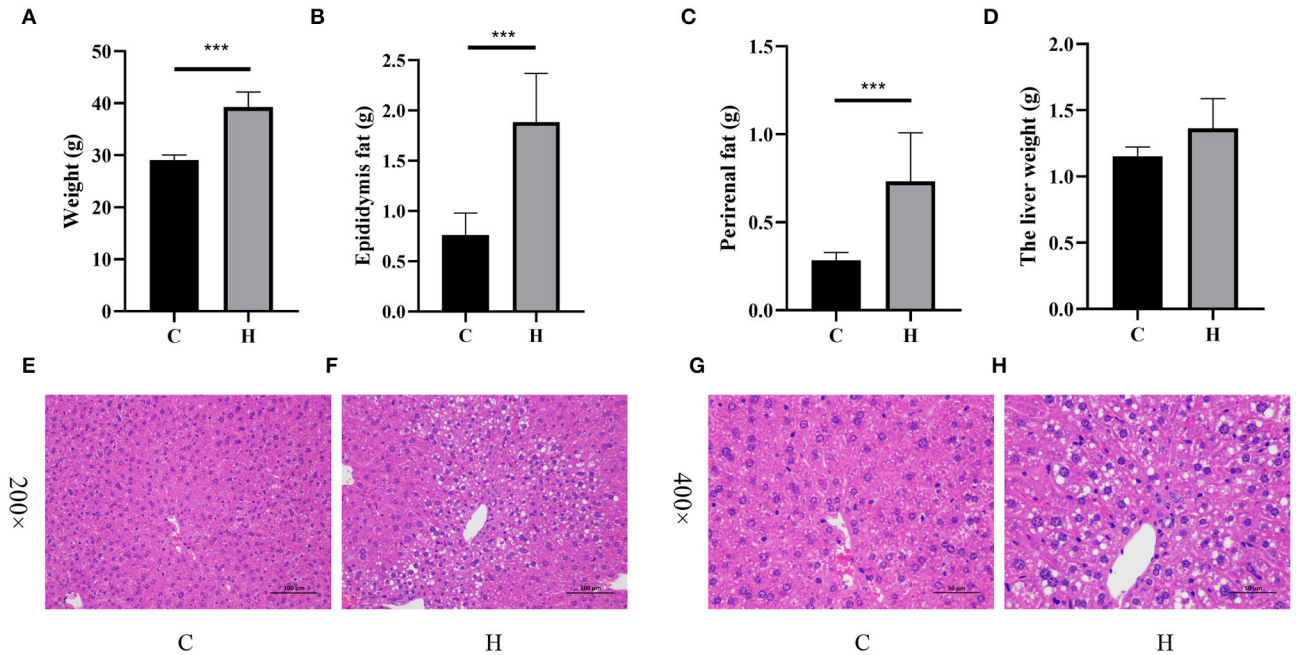

FIGURE 1 | High fructose corn syrup (HFCS) treatment affects body weight and fat deposition in mice. **(A)** Body weight of each group during the intervention period; **(B)** epididymal fat content in each group during the intervention period; **(C)** perirenal fat content in each group during the intervention period; **(D)** liver weight in each group during the intervention period; **(E)** the liver section was enlarged to 200× in Group C; and **(F)** the liver section was enlarged to 200× in Group H. **(G)** The liver section was enlarged to 400× in Group C and **(H)** the liver section was enlarged to 400× in Group H. ***$p < 0.001$.

TABLE 2 | Summary of the original data, clean data, sequencing error rate, clean read rate, and clean Q30 and Q20 base rate of the ordered samples.

Sample	raw_reads	clean_reads	clean_bases	Clean Q30 bases rate (%)	Mapped ratio (%)
C1	47,303,062	46,303,274	6.95G	94.80	94.06
C2	47,089,510	46,136,604	6.92G	94.13	93.48
C3	44,272,672	43,279,174	6.49G	94.43	93.85
C4	41,283,960	40,213,348	6.03G	94.40	92.99
C5	46,466,272	45,560,390	6.83G	94.69	93.80
H1	45,602,948	44,095,038	6.61G	94.75	93.34
H2	47,022,136	45,853,632	6.88G	94.56	95.24
H3	46,125,854	44,628,824	6.69G	94.67	93.72
H4	47,664,476	46,361,598	6.95G	94.62	95.05
H5	43,186,314	41,922,528	6.29G	94.67	93.84

was clear that the liver fat content in Group H was higher than that in Group C.

Differential Gene Expression Analysis

The Illumina HiSeq library was sequenced using the Illumina HiSeq platform to produce a paired-end reading of 150 bp. All sequencing data have been submitted to the NCBI Comprehensive Gene Expression Database with the registration number PRJNA731593. RNA from 10 samples was used, and the quality control method was mainly used to accurately detect RNA integrity with an Agilent 2100 Bioanalyzer. The results showed that the concentration and total amount of 10 samples met the requirements of sequencing. Ten samples were sequenced using the Hiseq 2500 high-throughput sequencing platform, and the average original reading of the 10 samples was 45,601,720. After removing the sequencing fitting and primer sequences, filtering the low-quality value data, and sequencing quality control, a total of 66.64 GB of clean

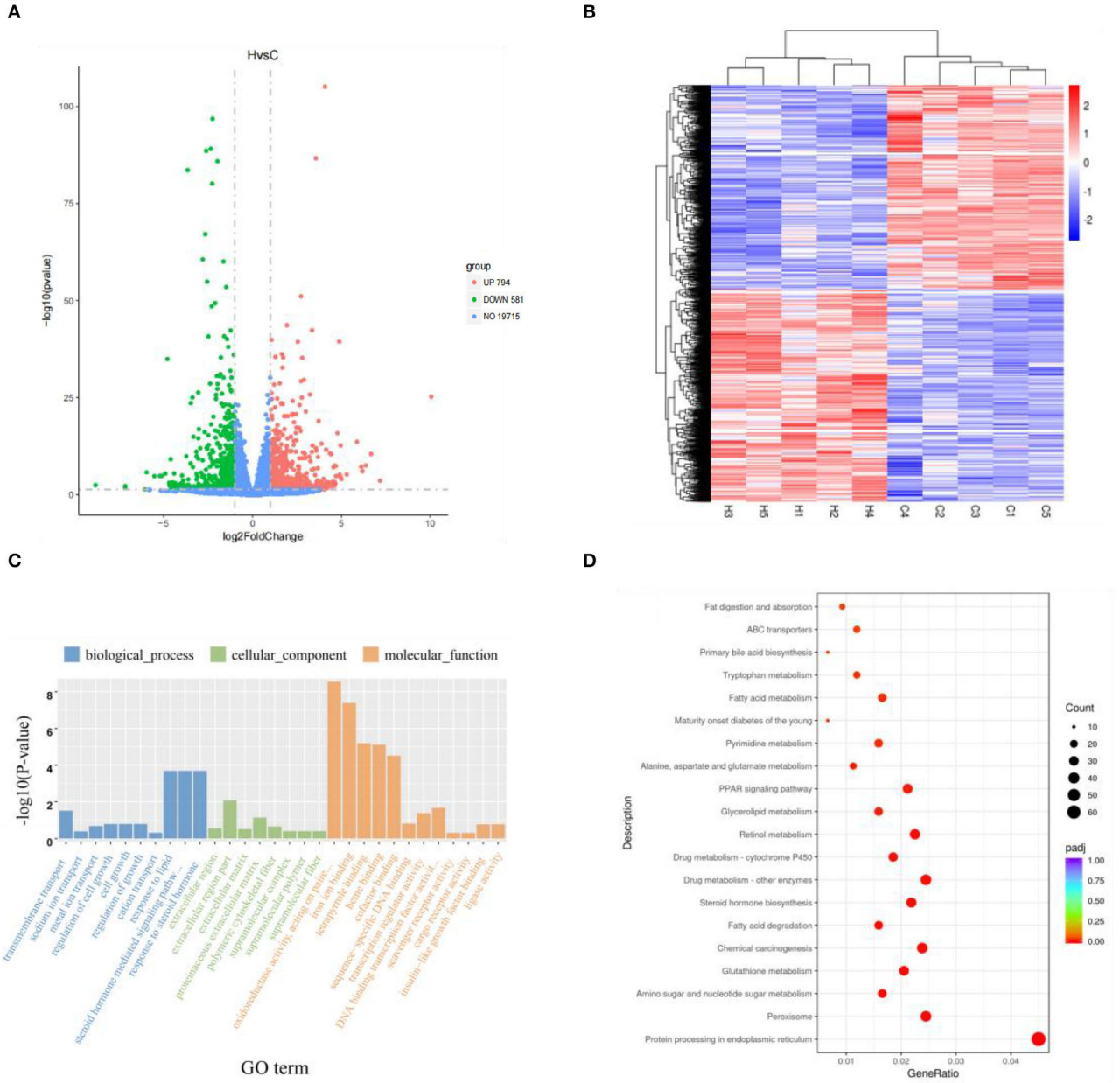

FIGURE 2 | Volcano map of total gene expression of Groups C and H. Red dots represent upregulated genes, green dots represent downregulated genes, and blue dots represent non-differentially expressed genes **(A)**. Expression profiles of 1,375 differentially expressed genes in liver tissue. Red represents upregulated genes, and blue represents downregulated genes **(B)**. Gee Oncology (GO) term enrichment analysis of differentially expressed genes **(C)**. KEGG pathway enrichment analysis of the first 20 differentially expressed genes obtained by Kyoto Encyclopedia of Genes and Genomes (KEGG) enrichment **(D)**.

data were obtained, and the average clean reading of the 10 samples was 44,435,441. In the clean data, Q30 is the percentage of the base with a recognition accuracy of over 99.9%; the reading proportion of the mass value over 30 (Q30) ranges from 94.13 to 94.8%; in the library, the content of gas chromatography ranges from 48.44 to 50.41% (**Table 2**), indicating good sequencing results.

A total of 21,090 genes were expressed in Groups C and H, with $p < 0.05$ and |log-2-fold change|> 1 as the threshold, and 1,375 DEGs were found. There were 794 upregulated genes and 581 downregulated genes in Group H when compared with Group C (**Figure 2A**). The DEG expression patterns of each sample were clustered on the basis of the log2 (fold change) values of their expression ratios, which exhibited good repeatability of samples in the two groups (**Figure 2B**).

To further elucidate the functional role of 1,375 DEGs, the GO and KEGG pathways were enriched to search for significant overabundance categories. GO terms were divided into three categories: biological processes, cell components, and molecular functions, and 47 terms ($p < 0.05$) were significantly enriched in the three categories. The first 30 terms were obtained through GO enrichment (that included 10 biological process terms, 8 molecular function terms, and 12 cellular component terms). Further analysis was performed to determine the relevant regulatory function (**Figure 2C**). Five terms were found to be related to lipid metabolism, including response to lipid (GO: 0033993), cellular response to lipid (GO: 0071396), response to steroid hormone (GO: 0048545), cellular response to steroid hormone stimulus (GO: 0071383), and steroid hormone-mediated signaling pathway (GO: 0043401). Five of these terms all belong to biological processes (**Table 3**).

A total of 1,375 DEGs were also integrated into the KEGG pathway database, and 32 pathways ($p < 0.05$) were significantly enriched. **Figure 2D** shows the first 20 significantly enriched pathways. Lipid metabolism and deposition involve five pathways, i.e., biosynthesis of unsaturated fatty acids pathway (mmu01040), steroid hormone biosynthesis (mmu00140) with 9 genes and 14 genes, 13 genes in peroxisome proliferator-activated receptors (PPAR) signaling pathway (mmu03320) and fatty acid elongation pathway (mmu00062) of 6 genes, tyrosine metabolism pathway (mmu00350) with 6 genes, and primary bile acid biosynthesis pathway (mmu00120) of 4 genes (**Table 4**). Combining GO and KEGG analysis, we screened 12 genes related to lipid metabolism (**Table 5**).

RT-QPCR Validation

To verify the RNA-Seq expression results, we further determined the expression level of 8 lipid-related genes in the liver of mice from Groups C and H, i.e., Stearoyl-Coenzyme A desaturase 1 (*Scd1*), *Pparg*, ELOVL Fatty Acid Elongase 3 (*Elovl3*), fatty acid desaturase 2 (*Fads2*), acyl-CoA thioesterase 2 (*Acot2*), acyl-CoA thioesterase 3 (*Acot3*), acyl-CoA thioesterase 4 (*Acot4*), and fatty acid binding protein 2 (*Fabp2*), of the eight genes. Only one was downregulated, and all the others were upregulated, using RT-qPCR analysis. These 8 genes related to growth metabolism were selected from the KEGG pathways and the GO terms that were significantly enriched in relation to lipid metabolism. Interestingly, these DEGs were all upregulated. Although the expression levels of these 8 determined genes in the liver were higher in Group C than in Group H, *Fabp2* was not significantly different ($p = 0.071$), and *Scd1*, *Pparg*, *Elovl3*, *Fads2*, *Acot2*, *Acot3*, and *Acot4* were genes that showed a significant ($p < 0.05$) difference between Groups C and H (**Figure 3**).

Differences in the Diversity and Composition of the Colon Microbiome in Mice

After 16SrRNA gene sequencing of colonic contents, the alpha diversity analysis structure indicated that Chao1 index, Shannon index and Simpson index indices were not significantly different ($P > 0.05$). It was shown that HFCS had no significant effect on the abundance of gut microbiota components in mice (**Figures 4A–C**). Beta diversity indicated that there was a large separation between Group C and Group H, indicating a considerable difference in gut microbial composition between the two groups (**Figure 4D**). To further investigate the effect of HFCS on intestinal microorganisms, we analyzed the microbial composition in the colon of mice in Groups C and H. Analysis of differences at the phylum level of the gut microbiome showed that when compared to Group C, the abundance of Proteobacteria and Actinobacteria was reduced in Group H. The abundance of Firmicutes was significantly reduced and Bacteroidetes was significantly increased in Group H. Analysis of differences at the genus level of the gut microbiome revealed that the abundances of *Allobaculum* and *Faecalibaculum* were significantly reduced, and the abundance of *Erysipelotrichaceae_uncultured*, *Parabacteroides,* and *Staphylococcus* was increased in Group H (**Figure 4E**).

Linear Discriminant Analysis Effect Size (LEfSe) Identified Different Bacteria Between Groups C and H

To further investigate the differences in the structure and abundance of mouse colonic bacteria at the level of 100 genera, heatmap analysis was performed on the differential genera obtained from LEfSe analysis. The results showed that there were obvious intergeneric differences in the colonic microbiome of mice. Under HFCS intervention, the relative abundance of *Bifidobacterium*, *Lactobacillus*, *Faecalibaculum*, *Erysipelatoclostridium,* and *Parasutterella* was increased in Group H, whereas the relative abundance of *Staphylococcus*, *Peptococcus*, *Parabacteroides*, *Donghicola,* and *Turicibacter* was reduced in Group H (**Figure 5**).

Correlation Analysis of Differentially Abundant Genera and Lipid Metabolism-Related Genes in Mice

Correlation analysis was performed to reveal the association between the gut microbiome and lipid metabolism-related genes. Through Spearman's correlation analysis, *Pparg*, *Acot2*, *Acot3,* and *Scd1* were positively correlated with *Erysipelatoclostridium* and negatively correlated with *Parabacteroides*, *Staphylococcus,*

TABLE 3 | The significantly enriched terms associated with lipid metabolism.

Term ID	Description	*p*-value	Gene number	Gene name
GO:0033993	response to lipid	0.035791763	6	*Rorc/Pparg/Nr3c2/Esrrg/Rxrg/Nr4a1*
GO:0043401	cellular response to lipid	0.035791763	6	*Rorc/Pparg/Nr3c2/Esrrg/Rxrg/Nr4a1*
GO:0048545	response to steroid hormone	0.035791763	6	*Rorc/Pparg/Nr3c2/Esrrg/Rxrg/Nr4a1*
GO:0071383	cellular response to steroid hormone stimulus	0.035791763	6	*Rorc/Pparg/Nr3c2/Esrrg/Rxrg/Nr4a1*
GO:0071396	steroid hormone mediated signaling pathway	0.035791763	6	*Rorc/Pparg/Nr3c2/Esrrg/Rxrg/Nr4a1*

TABLE 4 | The significantly enriched pathways associated with lipid metabolism.

Pathway ID	Description	*P* value	Gene number	Gene name
mmu01040	Biosynthesis of unsaturated fatty acids	0.000321506	9	*Elovl3/Fads2/Acot4/Acot3/Scd1/Acot2/Acnat2/Gm40474/Acot5*
mmu00140	Steroid hormone biosynthesis	0.00033063	14	*Cyp17a1/Cyp2b9/Cyp2c54/Ugt2b1/Cyp2c70/Cyp2c37/Ugt1a9/ Gm41857/Cyp2c38/Cyp2b13/Cyp7b1/Cyp2c39/Hsd3b5/Ugt2b38*
mmu03320	PPAR signaling pathway	0.001733084	13	*Ubc/Fads2/Cd36/Pparg/Fabp2/Cyp27a1/Pck2/ Cyp4a31/Scd1/Rxrg/Cyp4a14/Cyp4a12b/Plin1*
mmu00062	Fatty acid elongation	0.014560226	6	*Elovl3/Acot4/Acot3/Acot2/Gm40474/Acot5*
mmu00350	Tyrosine metabolism	0.019064803	6	*Got1/Aox3/Ddc/Adh7/Adh6-ps1/Aldh3a1*
mmu00120	Primary bile acid biosynthesis	0.020084289	4	*Cyp27a1/Cyp46a1/Acnat2/Cyp7b1*

TABLE 5 | Information of 12 differentially expressed genes associated with lipid metabolism.

Gene name	Gene ID	log2FoldChange	C readcount	H readcount	*P*-value	Descriptions
Pparg	19016	1.49	108.59	304.67	2.31E−15	peroxisome proliferator activated receptor gamma
Scd1	20249	1.19	64,638.17	147,212.05	1.09E−08	stearoyl-Coenzyme A desaturase 1
Rorc	19885	1.31	400.22	990.88	2.20E−14	RAR-related orphan receptor gamma
Fads2	56473	1.03	8,223.41	16,791.25	1.24E−22	fatty acid desaturase 2
Acot2	171210	1.93	307.2	1,170.6	1.96E−08	acyl-CoA thioesterase 2
Acot4	171282	1.41	631.39	1,674.93	2.05E−16	acyl-CoA thioesterase 4
Fabp2	14079	1.19	88.6	167.69	2.66E−13	fatty acid binding protein 2
Apoa4	11808	4.08	5,675.48	95,974.87	7.93E−106	apolipoprotein A-IV
Cyp46a1	13116	1.63	24.96	77.45	9.04E−09	cytochrome P450, family 46, subfamily a, polypeptide 1
Cyp27a1	104086	−1.01	5,987.95	2,970.2	5.74E−12	cytochrome P450 family 27 subfamily A member 1
Cyp7b1	13123	−1.43	4,090.27	1,520.04	0.0006842	cytochrome P450, family 7, subfamily b, polypeptide 1
Plin1	103968	−3.39	4.16	0.42	0.0419683	perilipin 1
Acot3	171281	2.12	386.94	1,682.7	2.120216	Acyl-CoA Thioesterase 3
Elovl3	12686	−2.61	9,921.82	1,628.4	2.71E−89	ELOVL Fatty Acid Elongase 3

Log2-foldchange of readcount by Group C (C readcount) vs. Group H (H readcount), of which 9 genes upregulated expression (log2-foldchange > 0) and 3 genes downregulated expression (log2-foldchange < 0).

and *Turicibacter*. *Bifidobacterium* was negatively correlated with *Elovl3* (**Figure 6**).

DISCUSSION

High fructose corn syrup is a syrupy mixture of glucose and fructose. In recent years, HFCS has been widely used in the food industry and has mostly replaced sucrose with the advantages of low price and better taste. Bocarsly (28) showed that a short-term intake of 8% HFCS increased body weight, along with increased abdominal fat in mice. These results suggest that HFCSs may have profound negative impacts on the liver and adipose tissue. HFCS alters body metabolism (3), and we found that HFCS intake affects intestinal microbes in a previous study (29). In the present study, we found that HFCS intake resulted in a significant increase in body weight and epididymal and perirenal fat in mice ($p < 0.001$). Although there was no significant difference in liver weight, observation of liver sections revealed that the proportion of lipid droplet area in liver tissue was greater in Group H than in Group C. Collectively, we thoroughly investigated mouse colonic microbes by 16S rRNA gene sequencing and analyzed changes in the abundance and

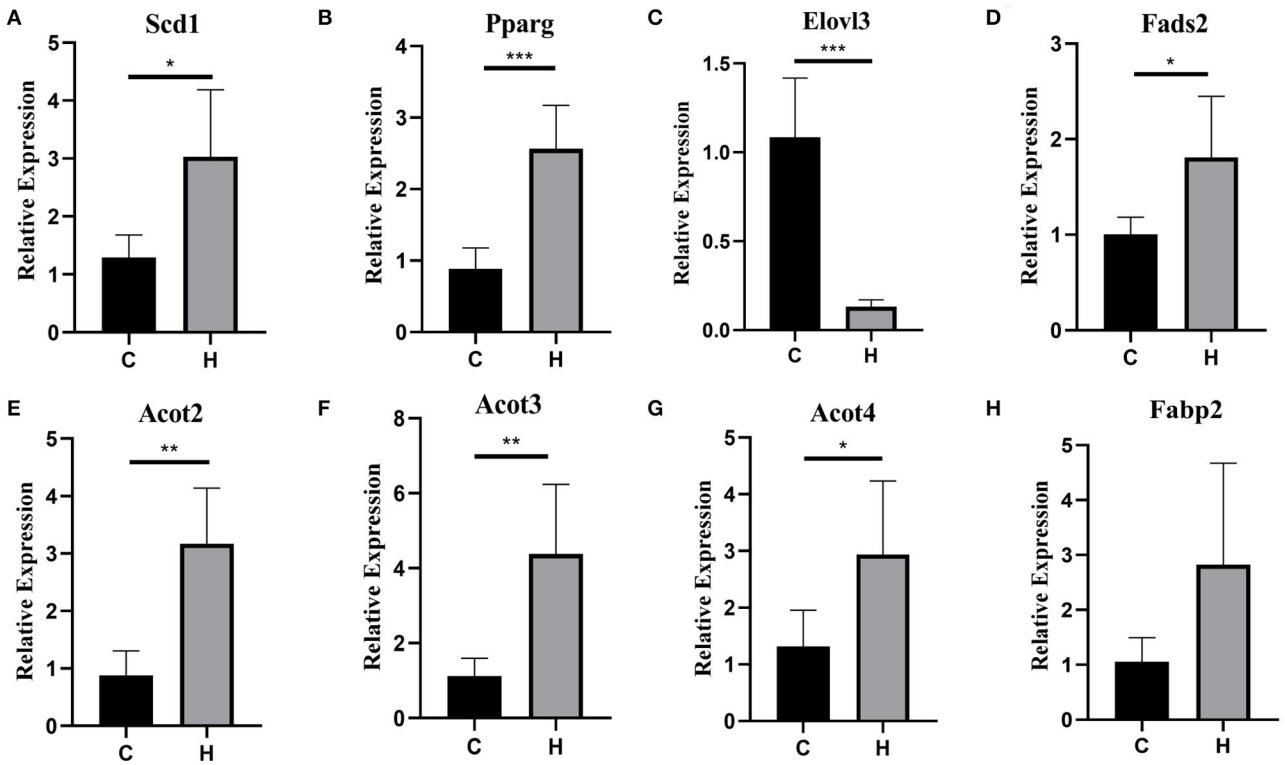

FIGURE 3 | (A–H) Validation of 8 differentially expressed genes (DEGs) between the groups C and H mice by RT-qPCR. The x-axis denotes the group, and the y-axis denotes the log2-fold change derived from RT-qPCR. $^{*}p < 0.05$, $^{**}p < 0.01$, $^{***}p < 0.001$.

structure of mouse colonic microbes after HFCS intervention. Not surprisingly, various bacteria existed in the mouse colon, with the dominant phyla being Bacteroidetes and Firmicutes, giving a result similar to other studies. Furthermore, we identified a total of 1,375 DEGs in the two groups by transcriptome analysis. Compared with Group C, we found 794 upregulated and 581 downregulated genes in Group H and found pathways related to lipid metabolism and inflammation. In addition, RT-PCR results showed that the expression of the *Elovl3* gene was reduced, while the other genes, such as *Scd1, Pparg, Fads2, Acot2, Acot3, Acot4, and Fabp2,* were all upregulated in Group H. Finally, this study shows that HFCS induces abnormalities in hepatic lipid metabolism and alters the structural abundance of the gut microbiome.

The liver is an important metabolic organ in the body that plays a role in deoxidation, storage of liver sugar, and synthesis of secreted proteins (30). Past studies have shown that one of the causes of obesity is the accumulation of individual lipids, which leads to a series of diseases (31). HFCS is considered to be more lipogenic than sucrose, which increases the risk for non-alcoholic fatty liver disease (NAFLD) and dyslipidemia (32). Similarly, in the present study, we found that the administration of HFCS induced higher liver fat infiltration and the most extensive fat blisters as compared to controls.

To better understand the mechanism by which HFCSs regulate hepatic lipid accumulation, further transcriptome sequencing was performed. There were 794 upregulated and 581 downregulated genes between the two groups, which were enriched in lipid metabolic pathways. In particular, the most significant difference observed regards the "biosynthesis of unsaturated fatty acids," which play multiple roles in human health (33). Functional analysis showed that the *Fabp2* and *Acot2* genes were related to liver regulation of lipid metabolism and IR through a series of biological processes (34). In the present study, the expression of *Acot2*, *Acot3*, and *Acot4* was significantly increased by HFCS treatment, suggesting that these three genes could promote adipocyte differentiation. *Elovl3* is known to promote fatty acid synthesis (lipogenesis), and RT-PCR results showed that the expression of the *Elovl3* gene was reduced. It was shown that the periodic expression of *Elovl3* in the liver may be controlled by the biological clock, related hormones, and transcription factors and confirmed that *Elovl3* has high and rhythmic expression in male mice (35). We speculate that the external environment may be a contributing factor in this phenomenon.

Peroxisome proliferator activated receptor gamma can control the peroxisome beta-oxidation pathway of fatty acids. Tontonoz et al. (36) reported that *Pparg* regulates adipocyte differentiation. The RT-PCR results showed that the expression of the *Pparg* gene was upregulated in Group H, and it is speculated that HFCS treatment increases the expression of *Pparg* and promotes

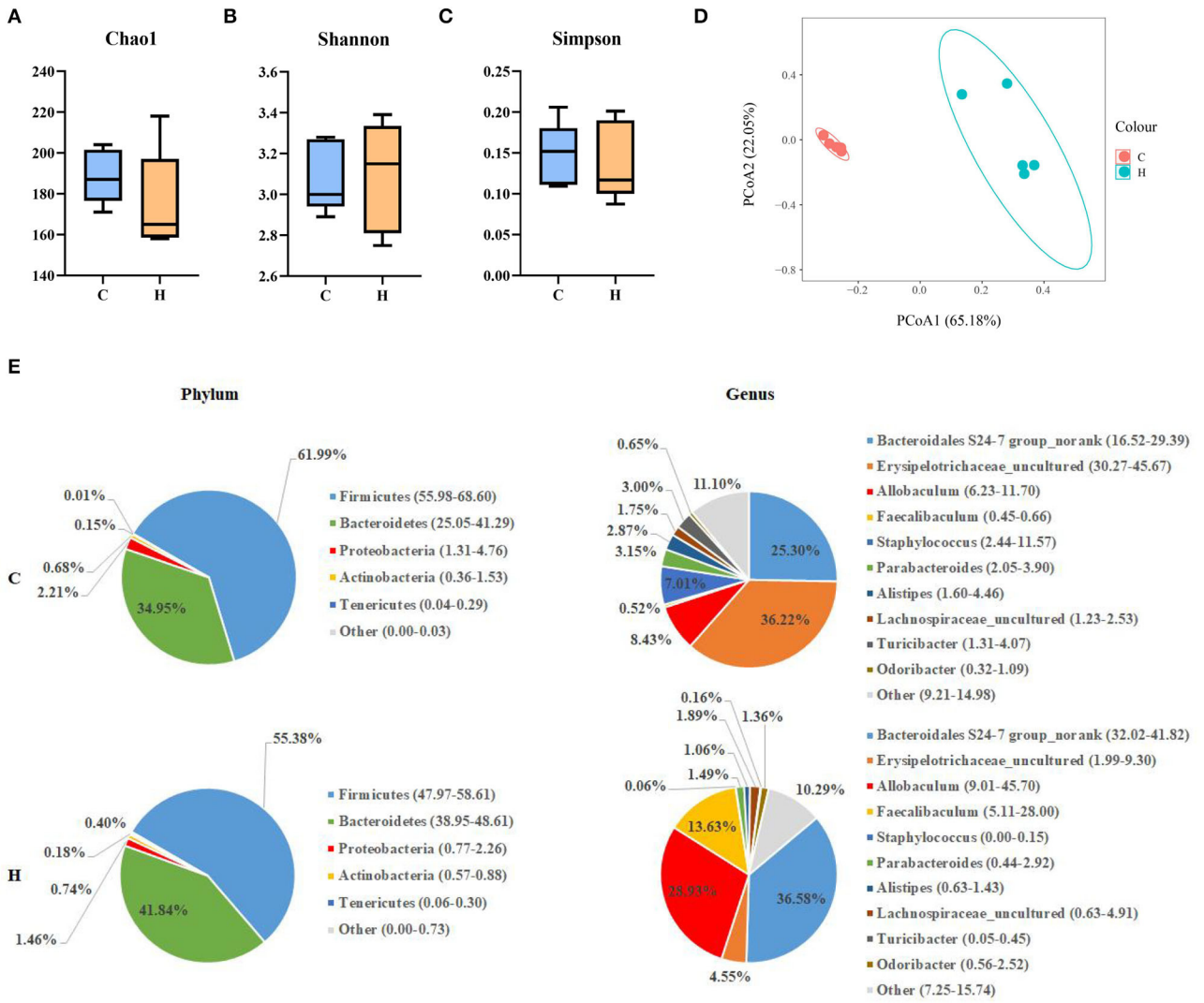

FIGURE 4 | Alpha diversity, including the Chao1 index, Shannon index, and Simpson index **(A–C)**. Principal coordinates analysis (PCoA) of the difference in the microbial community composition of 10 colons in mice. The percentages present the relative contribution of the 2 principal coordinates (PC1–PC2) **(D)**; phylum- and genus-level pie charts of the microbial composition in the colon of Groups C and H mice **(E)**.

the differentiation of adipocytes, which leads to the occurrence or aggravation of the individual obesity. Research shows that perilipin 1 (*Plin1*) expression is decreased in obese participants as compared to healthy controls (37). These findings demonstrate a novel role for *Plin* expression in adipose tissue metabolism and obesity regulation (38). *Fabp2* can help to maintain energy homeostasis by acting as a lipid sensor. *Fabp2* is a key factor in lipogenesis and lipid transport (34). In this study, we found that the *Fabp2* gene was enriched in the PPAR signaling pathway and that its expression was upregulated in Group H. Collectively, our findings suggested a functional role for *Pparg* and *Fabp2* in the regulation of HFCS-mediated hepatic lipid metabolism.

On the other hand, *Scd1* plays key roles in lipid storage, liposome homeostasis, and energy metabolism (39). The study of the *Scd1* gene mutant mouse strain provides evidence that *Scd1* is an important control point of lipid metabolism (40). Scd1-deficient mice had decreased liver fat content, suggesting the lack of *Scd1* protected mice from fat accumulation in the liver (41). This experiment revealed that the expression of *Scd1* was increased in the liver of mice by HFCS intervention, thus regulating the process of lipid metabolism, which is consistent with previous findings. In this study, Cytochrome P450 Family 27 Subfamily A Member 1 (*Cyp27a1*) and Cytochrome P450, Family 7, Subfamily b, Polypeptide 1 (*Cyp7b1*) were found to be reduced by HFCS intervention. Other studies have reported that Cyp27A1$^{-/-}$ mice have an enlarged liver and kidneys and increased triglyceride levels and fatty acid synthesis, and cholesterol absorption and synthesis (42). Furthermore, *Cyp7b1* has broad substrate specificity, is widely distributed in most organs, and plays important roles in the regulation of lipid

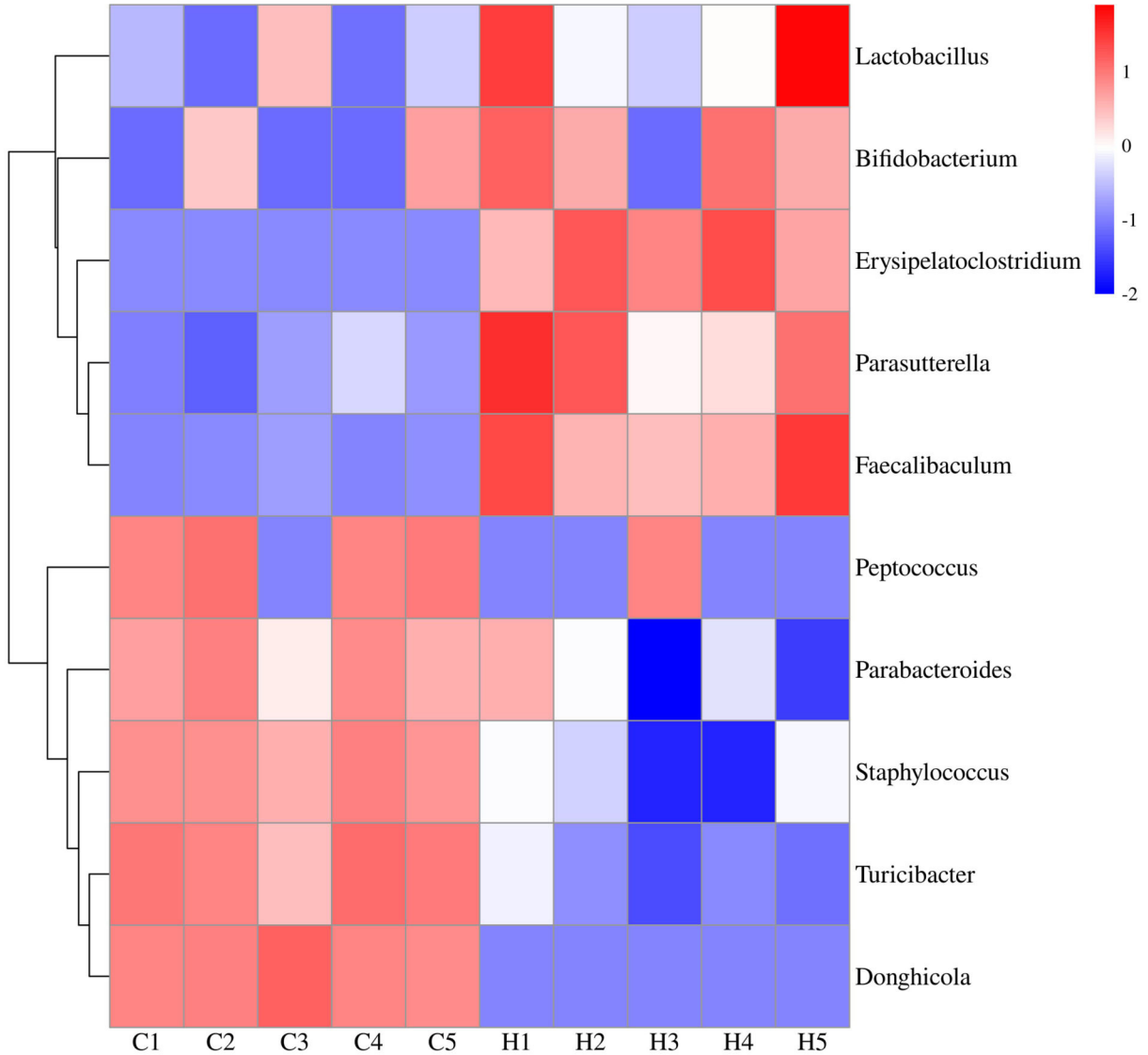

FIGURE 5 | Expression profiles of 10 differentially expressed bacteria in colonic contents. The vertical axis represents the genus clusters, and one row represents one genus. The color scale represents the expression abundance of the genera; red represents increased abundance, and blue represents decreased abundance.

metabolism (43). Overall, alterations in gene expression levels can affect lipid metabolism.

Many studies have shown that the gut microbiome plays an important role in determining body weight (44). PCoA representation of the bacterial genera composition of all samples revealed that HFCS intervention altered the mouse colon microbiome when compared with Group C. Our expectation was confirmed that specific bacteria would exist in the mouse colon, with the dominant phyla being Bacteroidetes and Firmicutes, a result consistent with other studies (45). In the present study, mice in Group H had a lower relative abundance of the Firmicutes phylum and a higher relative abundance of the Bacteroidetes phylum than mice in Group C. This result was confirmed by Mastrocola et al. (19), who found that the ratio of Firmicutes/Bacteroidetes and abundance of Firmicutes were decreased in mice fed fructose (20), which is consistent with our findings. In the present study, the relative abundance of *Bifidobacterium*, *Lactobacillus*, *Faecalibaculum*, *Erysipelatoclostridium,* and *Parasutterella* was increased after the HFCS diet as compared to the normal diet, as shown by the genus level of the heatmap, in contrast to the decrease in the relative abundance of *Staphylococcus*, *Peptococcus*, *Parabacteroides*, *Donghicola,* and *Turicibacter*. *Lactobacillus* remained tightly attached in the intestinal epithelium (46), and the abundance of *Lactobacillus* was increased with sugar intake (20). *Bifidobacterium* was increased only in mice fed the Western-style diet (WSD) + fructose diet, which is consistent with our findings. *Lactobacillus* and *Bifidobacterium*

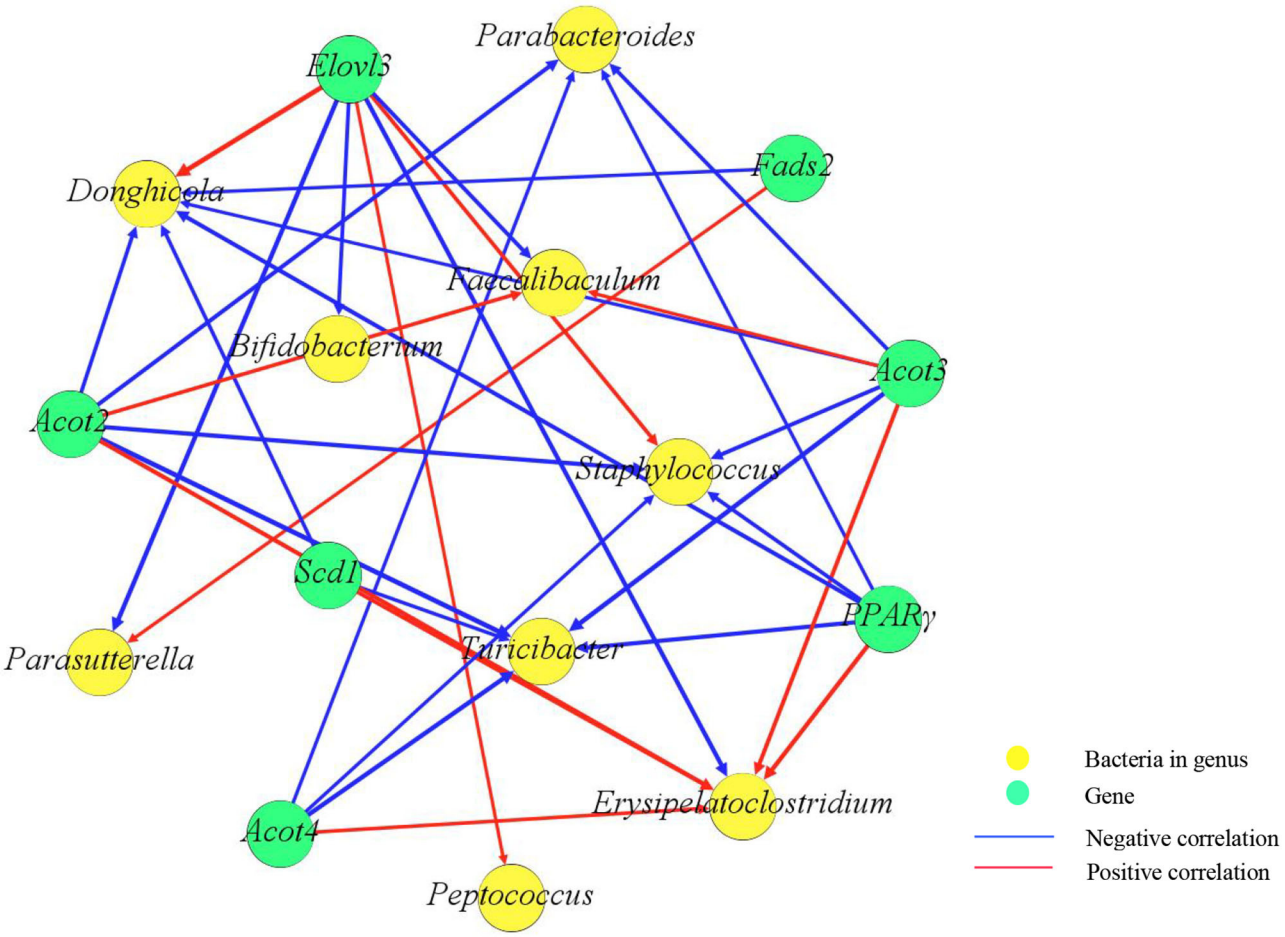

FIGURE 6 | Correlation network diagram between genes and the gut microbiome. Yellow spots represent bacteria, and green spots represent genes. Red lines represent positive correlations, and blue lines represent negative correlations. The weight of the lines represents the strength of the correlation, and the thicker the line is, the greater the absolute value of the correlation. The number of spots represents the number of correlated objects.

are considered to have health benefits, but some studies have found harmful effects on physical health (47, 48). *Parabacteroides* have an anti-obesity effect, Julia Beisner et al. found that they decreased after a high-fructose diet (19). Wang B et al. observed changes in intestinal microorganisms in mice through different diets and found that some studies showed a lower abundance of *Turicibacter* and *Pediococcus* in fructose diets than in controls (49).

Some studies have shown that the gut microbiome affects energy metabolism by regulating key genes (50). Erysipelotrichaceae has a positive correlation with obesity (51), and *Turicibacter* has been closely associated with abnormal lipid metabolism (52). *Parabacteroides* have an anti-obesity effect (45). *Pparg*, *Acot2,* and *Acot3* can promote adipocyte differentiation. It has been shown that the knockdown of Scd1 inhibits adipogenesis (53). *Scd1* can play a vital role in lipid metabolism, and its product oleic acid (OA) can promote lipolysis by upregulating lipase (54, 55). In this study, we found that *Pparg, Acot2, Acot3, and Scd1* were positively correlated with *Erysipelatoclostridium* and negatively correlated with *Turicibacter* and *Parabacteroides. Bifidobacterium* can suppress fat accumulation and regulate obesity and related metabolic diseases by affecting lipid metabolism (56–58). Elovl3 deletion may lead to reduced lipid accumulation in the liver (59). Our results showed that *Bifidobacterium* was positively correlated with *Pparg* and *Acot3* and negatively correlated with *Elovl3.* Overall, gut microbes can regulate related genes to influence lipid metabolism.

CONCLUSION

Our study demonstrated that HFCS intake resulted in a significant increase in body weight, epididymal and perirenal fat content, and an increase in the proportion of lipid droplet area in the liver, suggesting that HFCS may affect liver lipid metabolism in mice, leading to a lipid deposition. GO and KEGG analysis showed that *Pparg*, *Scd1*, RAR Related Orphan ReceptorC (*Rorc*), *Fads2*, *Acot2*, *Acot4*, *Fabp2*, apolipoprotein A-IV

(*Apoa4*), cytochrome P450, family 46, subfamily a,polypeptide1 (*Cyp46a1*), *Cyp27a1*, *Cyp7b1*, and *Plin1*, 12 genes were screened and found to display keyregulatory roles in lipidmetabolism. The PCR results contributed to elucidating the metabolic effect of HFCS in reducing the expression of *Elovl3* and increasing the expression of *Scd1, Pparg, Fads2, Acot2, Acot3, Acot4, and Fabp2* in sthe liver. At the phylum level, the HFCS diet increased the abundance of the Firmicutes phylum while decreasing the abundance of the Bacteroidetes phylum. Obviously, the Firmicutes/Bacteroidetes ratio also was reduced. At the genus level, the relative abundance of *Bifidobacterium*, *Lactobacillus*, *Faecalibaculum*, *Erysipelatoclostridium,* and *Parasutterella* was increased; in contrast, the relative abundance of *Staphylococcus*, *Peptococcus*, *Parabacteroides*, *Donghicola,* and *Turicibacter* was reduced by the HFCS diet. Correlation analysis indicated that *Pparg*, *Acot2*, *Acot3, and Scd1* were positively correlated with *Erysipelatoclostridium* and negatively correlated with *Turicibacter*. We conclude that HFCS has a significant impact on genes related to lipid metabolism in the liver and changes the structure and function of the colonic microbiome in mice; in particular, it decreases the abundance of bacteria with anti-obesity effects, which suggests that it may lead to disruption of intestinal function and thus affect the body's metabolism. In general, HFCS regulates the expression of lipid metabolism genes in the liver by affecting the gut microbiome, thereby influencing organismal metabolism.

DATA AVAILABILITY STATEMENT

The data presented in the study are deposited in the NCBI (National Center for Biotechnology Information) repository, accession numbers: PRJNA731593 and PRJNA826752.

ETHICS STATEMENT

The animal study was reviewed and approved by Zhejiang Provincial Ethics Committee for Laboratory Animals (Ethical Approval No.78865576).

AUTHOR CONTRIBUTIONS

YSh: methodology, review and editing, and data curation. YSu: methodology and review and editing. XW: methodology. YX: visualization. LM: supervision. WL: validation. ZZ: software. WW: funding acquisition, project administration, and resources. JL: conceptualization and investigation. All authors contributed to the article and approved the submitted version.

FUNDING

This research was supported by the State Key Laboratory for Managing Biotic and Chemical Threats to the Quality and Safety of Agroproducts, Grant/Award Number: 2010DS700124-ZZ2017.

ACKNOWLEDGMENTS

The authors would like to thank all members of the lab for their advice and technical assistance.

SUPPLEMENTARY MATERIAL

The Supplementary Material for this article can be found online at: https://www.frontiersin.org/articles/10.3389/fnut.2022.921758/full#supplementary-material

REFERENCES

1. Hanover LM, White JS. Manufacturing, composition, and applications of fructose. *Am J Clin Nutr*. (1993) 58:724S−32S. doi: 10.1093/ajcn/58.5.724S
2. Bray GA, Nielsen SJ, Popkin BM. Consumption of high-fructose corn syrup in beverages may play a role in the epidemic of obesity. *Am J Clin Nutr.* (2004) 79:537–43. doi: 10.1093/ajcn/79.4.537
3. Bhat SF, Pinney SE, Kennedy KM, McCourt CR, Mundy MA, Surette MG, et al. Exposure to high fructose corn syrup during adolescence in the mouse alters hepatic metabolism and the microbiome in a sex-specific manner. *J Physiol.* (2021) 599:1487–511. doi: 10.1113/JP280034
4. Diana CH, Mónica ST, Francisco LV. Miriam, Héctor L, Ricardo C, et al. Modulation of gut microbiota by Mantequilla and Melipona honeys decrease low-grade inflammation caused by high fructose corn syrup or sucrose in rats. *Food Res Int.* (2022) 151:110856. doi: 10.1016/j.foodres.2021.110856
5. Schultz A, Neil D, Aguila MB. Mandarim-de-Lacerda CA. Hepatic Adverse Effects of Fructose Consumption Independent of Overweight/Obesity. *Int J Mol Sci.* (2013) 14:21873–86. doi: 10.3390/ijms141121873
6. Reccia I, Kumar J, Akladios C, Virdis F, Pai M, Habib N, et al. Non-alcoholic fatty liver disease: a sign of systemic disease. *Metabolism.* (2017) 72:94–108. doi: 10.1016/j.metabol.2017.04.011
7. Fam BC, Joannides CN, Andrikopoulos S. The liver: Key in regulating appetite and body weight. *Adipocyte.* (2012) 1:259–64. doi: 10.4161/adip.21448
8. Li H, Wang T, Xu C, Wang D, Ren J, Li Y, et al. Transcriptome profile of liver at different physiological stages reveals potential mode for lipid metabolism in laying hens. *BMC Genom.* (2015) 16:763. doi: 10.1186/s12864-015-1943-0
9. Chon KS, Hoon KY, Wook SS, EunYi M, Suhkneung P, Hee US. Corrigendum to "Fisetin induces Sirt1 expression while inhibiting early adipogenesis in 3T3-L1 cells" [Biochem. Biophys. Res. Commun. 467(4) (2015) 638-644]. *Biochem Biophys Res Commun*. (2018) 506:306. doi: 10.1016/j.bbrc.2018.10.068
10. Pirany N, Balani AB, Hassanpour H, Mehraban H. Differential expression of genes implicated in liver lipid metabolism in broiler chickens differing in weight. *Br Poult Sci.* (2019) 61:10–6. doi: 10.1080/00071668.2019.1680802
11. Xu YY, Xu YS, Wang Y, Qin W, Shi JS. Dendrobium nobile Lindl. alkaloids regulate metabolism gene expression in livers of mice. *J Pharm Pharmacol.* (2017) 69:1409–17. doi: 10.1111/jphp.12778
12. Bourneuf E, Hérault F, Chicault C, Carré W, Assaf S, Monnier A, et al. Microarray analysis of differential gene expression in the liver of lean and fat chickens. *J Anim Sci Biotechnol.* (2006) 372:162–70. doi: 10.1016/j.gene.2005.12.028
13. D'Andre H, Paul W, Xu S, Jia X, Zhang R, Sun L, et al. Identification and characterization of genes that control fat deposition in chickens. *J Anim Sci Biotechnol.* (2014) 4:43. doi: 10.1186/2049-1891-4-43
14. Schoeler M, Caesar RJRiE, Disorders M. Dietary lipids, gut microbiota and lipid metabolism. *Rev Endocr Metab Disord.* (2019) 20:461–72. doi: 10.1007/s11154-019-09512-0

15. Velagapudi VR, Hezaveh R, Reigstad CS, Gopalacharyulu P, Yetukuri L, Islam S, et al. The gut microbiota modulates host energy and lipid metabolism in mice. *J Lipid Res.* (2010) 51:1101–12. doi: 10.1194/jlr.M002774
16. Sonnenburg JL, Bäckhed F. Diet–microbiota interactions as moderators of human metabolism. *Nature.* (2016) 535:56–64. doi: 10.1038/nature18846
17. Zhang YJ Li S, Gan RY, Zhou T, Xu DP Li HB. Impacts of Gut Bacteria on Human Health and Diseases. *Int J Mol Sci.* (2015) 16:7493–519. doi: 10.3390/ijms16047493
18. Xiao L, Estellé J, Kiilerich P, Ramayo-Caldas Y, Xia Z, Feng Q, et al. A reference gene catalogue of the pig gut microbiome. *Nat Microbiol.* (2016) 1:16161. doi: 10.1038/nmicrobiol.2016.161
19. Mastrocola R, Ferrocino I, Liberto E, Chiazza F, Cento AS, Collotta D, et al. Fructose liquid and solid formulations differently affect gut integrity, microbiota composition and related liver toxicity: a comparative in vivo study. *J Nutr Biochem*. (2018) 55:185–99. doi: 10.1016/j.jnutbio.2018.02.003
20. Noble EE, Hsu TM, Jones RB, Fodor AA. Kanoski SE. Early-Life Sugar Consumption Affects the Rat Microbiome Independently of Obesity. *J Nutr.* (2017) 147:20–8. doi: 10.3945/jn.116.238816
21. Crescenzo R, Mazzoli A, Luccia BD, Bianco F, Cancelliere R, Cigliano L, et al. Dietary fructose causes defective insulin signalling and ceramide accumulation in the liver that can be reversed by gut microbiota modulation. *Food Nutr Res.* (2017) 61:1331657. doi: 10.1080/16546628.2017.1331657
22. Minoru K, Michihiro A, Susumu G, Masahiro H, Mika H, Masumi I, et al. KEGG for linking genomes to life and the environment. *Nucleic Acids Res.* (2008) 36:D480–4. doi: 10.1093/nar/gkm882
23. Mao X, Tao C, Olyarchuk JG, Wei L. Automated genome annotation and pathway identification using the KEGG Orthology (KO) as a controlled vocabulary. *Bioinformatics.* (2005) 21:3787–93. doi: 10.1093/bioinformatics/bti430
24. Zheng Z, Xiao Y, Ma L, Lyu W, Peng H, Wang X, et al. Low dose of sucralose alter gut microbiome in mice. *Front Nutr.* (2022) 9:848392. doi: 10.3389/fnut.2022.848392
25. Lawley B, Tannock GW. Analysis of 16S rRNA gene amplicon sequences using the QIIME software package. *Methods Mol Biol.* (2017) 1537:153–63. doi: 10.1007/978-1-4939-6685-1_9
26. Magoč T, Salzberg SL. FLASH: fast length adjustment of short reads to improve genome assemblies. *Bioinformatics.* (2011) 27:2957–963. doi: 10.1093/bioinformatics/btr507
27. Wang Q. Naive Bayesian classifier for rapid assignment of rRNA sequences into the new bacterial taxonomy. *Appl Environ Microbiol.* (2007) 73:5261–7. doi: 10.1128/AEM.00062-07
28. Bocarsly ME. High-fructose corn syrup causes characteristics of obesity in rats: increased body weight, body fat and triglyceride levels. *Pharmacol Biochem Behav.* (2010) 97:101–6. doi: 10.1016/j.pbb.2010.02.012
29. Han X, Feng Z, Chen Y, Zhu L, Li X, Wang X, et al. Effects of high-fructose corn syrup on bone health and gastrointestinal microbiota in growing male mice. *Front Nutr.* (2022) 9:829396. doi: 10.3389/fnut.2022.829396
30. Sahini N, Borlak J. Recent insights into the molecular pathophysiology of lipid droplet formation in hepatocytes. *Prog Lipid Res.* (2014) 54:86–112. doi: 10.1016/j.plipres.2014.02.002
31. Sipka S, Bruckner G. The Immunomodulatory Role of Bile Acids. *Int Arch Allergy Immunol*. (2014) 165:1–8. doi: 10.1159/000366100
32. Mock K, Lateef S, Benedito VA, Tou JC. High-fructose corn syrup-55 consumption alters hepatic lipid metabolism and promotes triglyceride accumulation. *J Nutr Biochem.* (2017) 39:32–9. doi: 10.1016/j.jnutbio.2016.09.010
33. Brenner, Rodolfo R. Antagonism between Type 1 and Type 2 diabetes in unsaturated fatty acid biosynthesis. *Future Lipidol.* (2006) 1:631–40. doi: 10.2217/17460875.1.5.631
34. Hu G, Wang S, Tian J, Chu L, Li H. Epistatic effect between ACACA and FABP2 gene on abdominal fat traits in broilers - ScienceDirect. *J Genet Genomics*. (2010) 37:505–12. doi: 10.1016/S1673-8527(09)60070-9
35. Chen H, Lei G, Dan Y, Xiao Y, Jin Y. Coordination between the circadian clock and androgen signaling is required to sustain rhythmic expression of Elovl3 in mouse liver. *J Biol Chem.* (2019) 294:7046–56. doi: 10.1074/jbc.RA118.005950
36. Tontonoz P, Hu E, Spiegelman BM. Stimulation of adipogenesis in fibroblasts by PPAR gamma 2, a lipid-activated transcription factor. *Cell.* (1994) 79:1147–56. doi: 10.1016/0092-8674(94)90006-X
37. Ylmaz EG, Bozkurt H. Ndad za A, Thomford NE, Dandara C. Childhood Obesity Risk in Relationship to Perilipin 1 (PLIN1) Gene Regulation by Circulating microRNAs. *OMICS.* (2020) 24:43–50. doi: 10.1089/omi.2019.0150
38. Miyoshi H, Souza SC, Endo M, Sawada T, Perfield JW, Shimizu C, et al. Perilipin overexpression in mice protects against diet-induced obesity. *J Lipid Res.* (2010) 51:975–82. doi: 10.1194/jlr.M002352
39. Thumser AE, Moore JB, Plant NJ. Fatty acid binding proteins: tissue-specific functions in health and disease. *Curr Opin Clin Nutr Metab Care.* (2014) 17:124–9. doi: 10.1097/MCO.0000000000000031
40. Dobrzyn A, Ntambi JM. The role of stearoyl-CoA desaturase in the control of metabolism. *Prostaglandins Leukot Essent Fatty Acids.* (2005) 73:35–41. doi: 10.1016/j.plefa.2005.04.011
41. Cohen P. Role for Stearoyl-CoA Desaturase-1 in Leptin-Mediated Weight Loss. *Science.* (2002) 297:240–3. doi: 10.1126/science.1071527
42. Repa JJ, Lund EG, Horton JD, Leitersdorf E, Russell DW, Dietschy JM, et al. Disruption of the Sterol 27-Hydroxylase Gene in Mice Results in Hepatomegaly and Hypertriglyceridemia: Reversal by cholic acid feeding. *J Biol Chem*. (2000) 275:39685–92. doi: 10.1074/jbc.M007653200
43. Chiang JYL. Regulation of bile acid synthesis: pathways, nuclear receptors, and mechanisms. *J Hepatol.* (2004) 40:539–51. doi: 10.1016/j.jhep.2003.11.006
44. Cardinelli CS, Sala PC, Alves CC, Torrinhas RS, Waitzberg DL. Influence of intestinal microbiota on body weight gain: a narrative review of the literature. *Obes Surg.* (2015) 25:346–53. doi: 10.1007/s11695-014-1525-2
45. Beisner J, Gonzalezgranda A, Basrai M, Dammsmachado A, Bischoff SC. Fructose-induced intestinal microbiota shift following two types of short-term high-fructose dietary phases. *Nutrients.* (2020) 12:3444. doi: 10.3390/nu12113444
46. Karczewski J, Troost FJ, Konings I, Dekker J, Wells JM. Regulation of human epithelial tight junction proteins by Lactobacillus plantarum in vivo and protective effects on the epithelial barrier. *Am J Physiol Gastrointest Liver Physiol.* (2010) 298:G851–9. doi: 10.1152/ajpgi.00327.2009
47. Gois M, Sinha T, Spreckels JE, Vila AV, Kurilshikov A. Role of the gut microbiome in mediating lactose intolerance symptoms. *Gut.* (2022) 71:215–7. doi: 10.1136/gutjnl-2020-323911
48. Pararajasingam A, Uwagwu J. Lactobacillus: the not so friendly bacteria. *BMJ Case Rep*. (2017) 2017:bcr2016218423. doi: 10.1136/bcr-2016-218423
49. Wang B, Gao R, Wu Z, Yu Z. Functional Analysis of Sugars in Modulating Bacterial Communities and Metabolomics Profiles of Medicago sativa Silage. *Front Microbiol.* (2020) 11:641. doi: 10.3389/fmicb.2020.00641
50. Backhed F, Ding H, Wang T, Hooper LV, Koh GY, Nagy A, et al. The gut microbiota as an environmental factor that regulates fat storage. *Proc Natl Acad Sci USA*. (2004) 101:15718–23. doi: 10.1073/pnas.0407076101
51. Ye J, Zhao Y, Chen X, Zhou H, Xiao M. Pu-erh tea ameliorates obesity and modulates gut microbiota in high fat diet fed mice. *Food Res Int.* (2021) 144:110360. doi: 10.1016/j.foodres.2021.110360
52. Li C, Zhang Y, Ge Y, Qiu B. Tao H. Comparative transcriptome and microbiota analyses provide new insights into the adverse effects of industrial trans fatty acids on the small intestine of C57BL/6 mice. *Eur J Nutr.* (2021) 60:975–87. doi: 10.1007/s00394-020-02297-y
53. Ntambi JM, Miyazaki M, Stoehr JP, Lan H, Kendziorski CM, Yandell BS, et al. Loss of stearoyl-CoA desaturase-1 function protects mice against adiposity. *Proc Natl Acad Sci USA*. (2002) 99:11482–6. doi: 10.1073/pnas.132384699

54. Zou Y, Wang YN, Ma H, He ZH, Tang Y, Guo L. et al. SCD1 promotes lipid mobilization in subcutaneous white adipose tissue. *J Lipid Res.* (2020) 61:1589–604. doi: 10.1194/jlr.RA120000869
55. Ravaut G, Légiot A, Bergeron KF, Mounier C. Monounsaturated fatty acids in obesity-related inflammation. *Int J Mol Sci.* (2020) 22:330. doi: 10.3390/ijms22010330
56. Yamamura R, Okubo R, Katsumata N, Odamaki T, Hashimoto N, Kusumi I, et al. Lipid and energy metabolism of the gut microbiota is associated with the response to probiotic bifidobacterium breve strain for anxiety and depressive symptoms in schizophrenia. *J Pers Med.* (2021) 11:987. doi: 10.3390/jpm11100987
57. Kikuchi K, Ben Othman M, Sakamoto K. Sterilized bifidobacteria suppressed fat accumulation and blood glucose level. *Biochem Biophys Res Commun*. (2018) 501:1041–7. doi: 10.1016/j.bbrc.2018.05.105
58. Sun Y, Tang Y, Hou X, Wang H, Science YBJFiV. Novel Lactobacillus reuteri HI120 Affects Lipid Metabolism in C57BL/6 Obese Mice. *Front Vet Sci.* (2020) 7:560241. doi: 10.3389/fvets.2020.560241
59. Zadravec D, Brolinson A, Fisher RM, Carneheim C, Csikasz RI, Bertrand-Michel J, et al. Ablation of the very-long-chain fatty acid elongase ELOVL3 in mice leads to constrained lipid storage and resistance to diet-induced obesity. *FASEB J.* (2010) 24:4366–77. doi: 10.1096/fj.09-152298

Conflict of Interest: The authors declare that the research was conducted in the absence of any commercial or financial relationships that could be construed as a potential conflict of interest.

Publisher's Note: All claims expressed in this article are solely those of the authors and do not necessarily represent those of their affiliated organizations, or those of the publisher, the editors and the reviewers. Any product that may be evaluated in this article, or claim that may be made by its manufacturer, is not guaranteed or endorsed by the publisher.

Copyright © 2022 Shen, Sun, Wang, Xiao, Ma, Lyu, Zheng, Wang and Li. This is an open-access article distributed under the terms of the Creative Commons Attribution License (CC BY). The use, distribution or reproduction in other forums is permitted, provided the original author(s) and the copyright owner(s) are credited and that the original publication in this journal is cited, in accordance with accepted academic practice. No use, distribution or reproduction is permitted which does not comply with these terms.